

Supporting Information

For

First example of Cu(I)-(η^2 -O,O)nitrite complex derived from Cu(II)-nitrosyl

Apurba Kalita, Pankaj Kumar, Ramesh C. Deka and Biplab Mondal*

Department of Chemistry, Indian Institute of Technology Guwahati, Assam 781039, India

Table of Contents

Sl. No.	Content	Page No.
1	Experimental Section	02
2	Figure S1: ORTEP diagram of complex 1	06
3	Figure S2: ORTEP diagram of complex 3	06
4	Figure S3: FT-IR spectrum of L in KBr	07
5	Figure S4: $^1\text{H-NMR}$ spectrum of L in methanol- d_4	07
6	Figure S5: $^{13}\text{C-NMR}$ spectrum of L in methanol- d_4	08
7	Figure S6: ESI-mass spectrum of L in methanol	08
8	Figure S7: FT-IR spectrum of complex 1 in KBr	09
9	Figure S8: $^1\text{H-NMR}$ spectrum of complex 1 in CD_3CN	09
10	Figure S9: ESI-Mass spectrum of complex 1 in methanol.	10
11	Figure S10: X-band EPR spectra of the complexes 1 (black) and 2 (red) in acetonitrile at 77 K	10
12	Figure S11: UV-visible spectra of complexes 1 (red) and 2 (blue) in acetonitrile solvent at room temperature	11
13	Figure S12: UV-visible spectrum of complex 2 in acetonitrile solvent at room temperature	11
14	Figure S13: FT-IR spectrum of complex 2 in KBr	12
15	Figure S14: FT-IR spectra of complex 2 derived from nitric oxide (black) and ^{15}NO (blue) in acetonitrile solution.	12
16	Figure S15: $^1\text{H-NMR}$ spectrum of complex 2 in methanol- d_4	13
17	Figure S16: ESI-Mass spectrum of complex 2 in acetonitrile.	13
18	Figure S17: FT-IR spectrum of complex 3 in KBr	14
19	Figure S18: UV-visible spectrum of complex 3 in acetonitrile solvent at room temperature	14
20	Figure S19: (a) UV-visible spectroscopic monitoring of the reaction of complex 2 with water in acetonitrile.	15
21	Figure S20: Solution FT-IR spectra of complex 2 (red line) and after reaction with water in acetonitrile solvent at room temperature	15
22	Figure S21: ESI-mass spectrum of complex 3 obtained from the reaction of complex 2 and water in acetonitrile	16
23	Figure S22: ESI-mass spectrum of complex 3 obtained from the reaction of complex 2 and water (^{18}O -labeled) in acetonitrile	16
24	Figure S23: $^1\text{H-NMR}$ spectrum of complex 3 in methanol- d_4	17
25	Table S1. Crystallographic data for complex 1 and 3	17
26	Table S2. Selected bond length (Å) for complex 1 and 3	18
27	Table S3. Selected bond angles ($^\circ$) for complex 1 and 3	18

Experimental Section

General:

All reagents and solvents were purchased from commercial sources and were of reagent grade. Acetonitrile was distilled from calcium hydride. Deoxygenation of the solvent and solutions were effected by repeated vacuum/purge cycles or bubbling with nitrogen for 30 minutes. NO gas was purified by passing through KOH and P₂O₅ column. UV-visible spectra were recorded on a Perkin Elmer Lambda 25 UV-visible spectrophotometer. FT-IR spectra were taken on a Perkin Elmer spectrophotometer with samples prepared either as KBr pellets or for solutions, in NaCl cell of one cm path length. Solution electrical conductivity was checked using a Systronic 305 conductivity bridge. ¹H-NMR spectra were obtained with a 400 MHz Varian FT spectrometer. Chemical shifts (ppm) were referenced either with an internal standard (Me₄Si) for organic compounds or to the residual solvent peaks. The X-band Electron Paramagnetic Resonance (EPR) spectra of the complexes and of the reaction mixtures were recorded on a JES-FA200 ESR spectrometer. Elemental analyses were obtained from a Perkin Elmer Series II Analyzer. The magnetic moment of complexes are measured on a Cambridge Magnetic Balance. Single crystals were grown by slow diffusion followed by slow evaporation technique. The intensity data were collected using a Bruker SMART APEX-II CCD diffractometer, equipped with a fine focus 1.75 kW sealed tube MoK α radiation ($\lambda = 0.71073 \text{ \AA}$) at 296(2)K with increasing ω (width of 0.3° per frame) at a scan speed of 3 s/frame. The SMART software was used for data acquisition. Data integration and reduction were undertaken with SAINT and XPREP software. Structures were solved by direct methods using SHELXS-97 and refined with full-matrix least squares on F^2 using SHELXL-97.

All non-hydrogen atoms were refined anisotropically. Structural illustrations have been drawn with ORTEP-3 for Windows.

DFT calculations were performed on complex **2**. The complex was fully optimized using PW91 functional and DNP basis sets in the presence of solvent acetonitrile. The Conductor-like Screening Model (COSMO) as incorporated into the DMol³ program with dielectric constant of 37.5 was adopted to study the solvent effect.^{2,3} The HOMO and LUMO energy values were also calculated in the presence of solvent and they are shown in S29 and S30, respectively. It has been observed that both HOMO and LUMO orbitals are localized on the imidazole ring of the ligand. NBO calculations were performed on the optimized cluster to identify the electronic distribution on the complex.

Synthesis of ligand, L

The ligand **L** was synthesized by a method adapted from Morteza Shiri.¹

A 100-ml, two-necked, round-bottomed flask equipped with a magnetic stirring bar, and a rubber septum was charged with 2.20g (20 mmol) of 2-ethyl-4-methyl-imidazole, and 30 mL of methanol. To the stirred solution 0.45g (15 mmol) of formaldehyde was added over a period of 5 min and the resulting mixture was made alkaline (pH ~14) by adding KOH. The reaction mixture was then allowed to stir. at room temperature . After 3-4 hr. Ligand **L**₁ comes out from the reaction mixture as white precipitate .The white precipitate was washed with water, dried in vacuum. Yield: 1.97 g (85%). It was characterized by elemental analysis, FT-IR, ¹H- NMR and ¹³C-NMR spectroscopy. Elemental analyses: Calcd. (%) for C₁₃H₂₀N₄: C, 67.21; H, 8.68; N, 24.12. Found (%): C, 67.19; H, 8.68; N, 24.02. FT-IR (in KBr): 2964, 2842, 1614, 1529, 1455, 1071 cm⁻¹; ¹H-NMR (400 MHz,

CDCl_3): δ_{ppm} , 3.53(2H), 2.44(4H), 1.87(6H), 1.08(6H). $^{13}\text{C-NMR}$ (100 MHz, CDCl_3):
 δ_{ppm} , 149.17, 129.09, 127.15, 23.29, 22.55, 13.66, 10.64. Mass: (m+H⁺)/z: Calcd. 233.16;
Found, 233.17.

Synthesis of complex 1, $[\text{Cu}(\text{L})_2](\text{ClO}_4)_2$

Hexaaquacopper(II)perchlorate (0.740 g, 2 mmol) was dissolved in 20 ml distilled methanol. To this solution, 0.928 g (4 mmol) of the ligand **L** was added slowly with constant stirring. The color of the solution turned into dark brown from light blue. The stirring was continued for 1h at room temperature. The volume of the solution then reduced to ~5 ml. To this, 10 ml of diethylether was added to make a layer on it and kept it overnight on freezer. This resulted into microcrystalline complex **1**. Yield: 1.25 g (85%). Elemental Analyses: Calcd. for $\text{C}_{26}\text{H}_{40}\text{Cl}_2\text{CuN}_8\text{O}_8$: C, 42.95; H, 5.55; N, 15.41. Found (%): C, 42.91; H, 5.54; N, 15.36. FT-IR: 2976, 1633, 1455, 1150, 1114, 625cm^{-1} ; magnetic moment, 1.60 BM. ESI-Mass: 527.24. CCDC No. 838636.

Synthesis of complex 2, $[\text{Cu}(\text{L})_2(\text{NO})](\text{ClO}_4)_2$

To 20 ml of distilled and degassed acetonitrile solution of complex **1** (500 mg), freshly prepared nitric oxide was bubbled for 1 minute. The color of the solution turned dark green. The excess of nitric oxide was removed by vacuum and purging argon gas and 10 ml of degassed benzene was added to this under nitrogen atmosphere. The reaction mixture was kept in freezer for two days. This resulted into the precipitate of complex **2** as green powder. Yield: 0.364 g (70%). Elemental Analyses: Calcd. for

$C_{26}H_{40}Cl_2CuN_9O_9$: C, 41.25; H, 5.32; N, 16.65. Found (%): C, 41.28; H, 5.30; N, 16.70.

FT-IR (in KBr): 2921, 1662, 1620, 1475, 1384, 1242, 1108, 625 cm^{-1} . ESI-Mass: 557.46.

Synthesis of complex 3, [Cu (L)₂(NO₂)]

To 15 ml of distilled and degassed acetonitrile solution of complex **2** (500 mg) quantitative amount of distilled water was added at room temperature with constant stirring under nitrogen environment. The green color of the solution turned colorless. It was kept on freezer. After three days, yellow color crystals of complex **3** were obtained. Yield: 0.265 g (63%). Elemental Analyses: Calcd. for $C_{26}H_{40}CuN_9O_2$: C, 54.38; H, 7.02; N, 21.95. Found (%): C, 54.36; H, 7.04; N, 21.91. FT-IR(in KBr): 2976, 1639, 1535, 1455, 1377, 1322, 1267, 1175, 967, 789 cm^{-1} . ESI-Mass: 573.26 (when water used to prepare the complex) and 575.21 (when ^{18}O -labeled water was used). CCDC No. 838637.

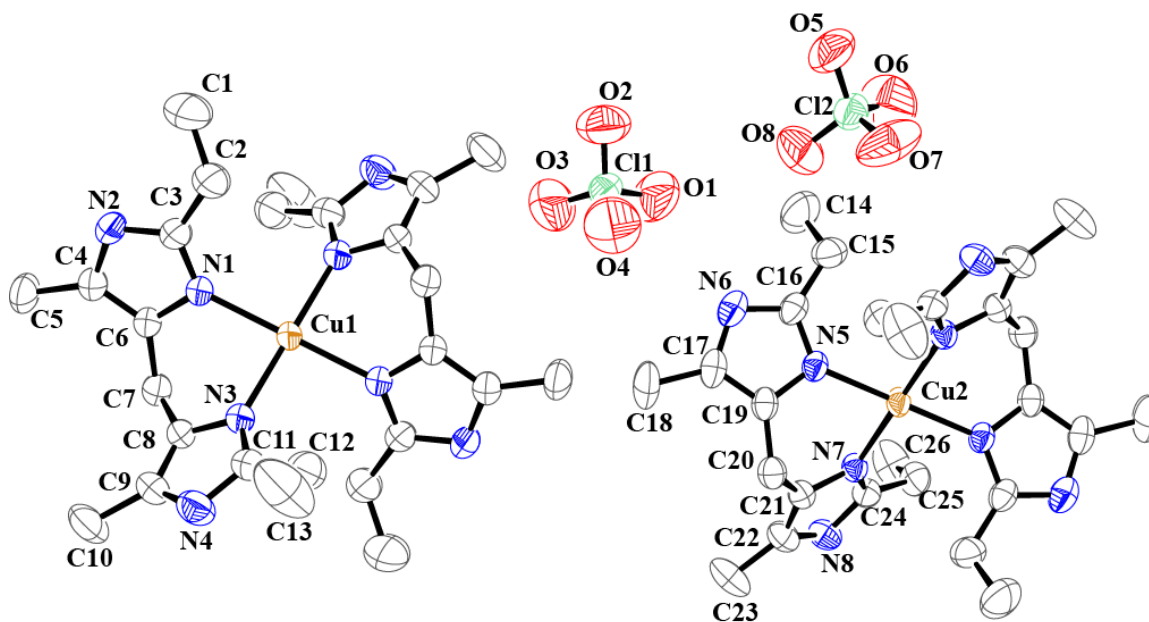


Figure S1. ORTEP diagram of complex **1** (50% thermal ellipsoid plot) (Hydrogen atoms and acetonitrile solvent are omitted for clarity).

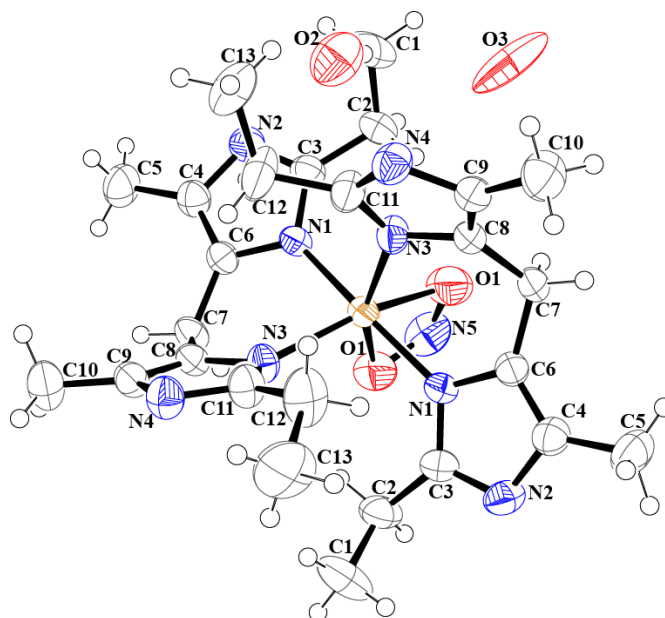


Figure S2. ORTEP diagram of complex **3** (50% thermal ellipsoid plot).

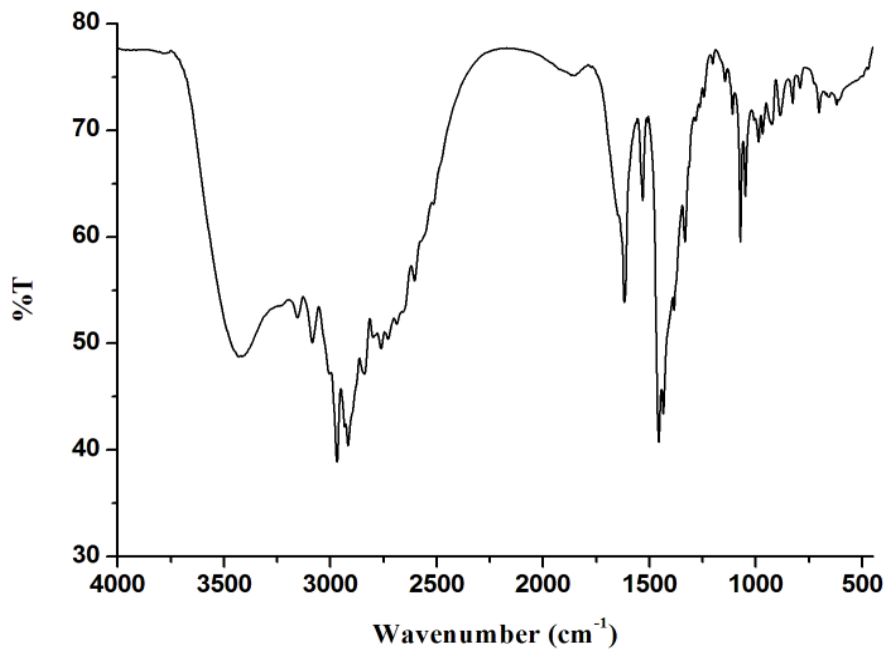


Figure S3: FT-IR spectrum of **L** in KBr.

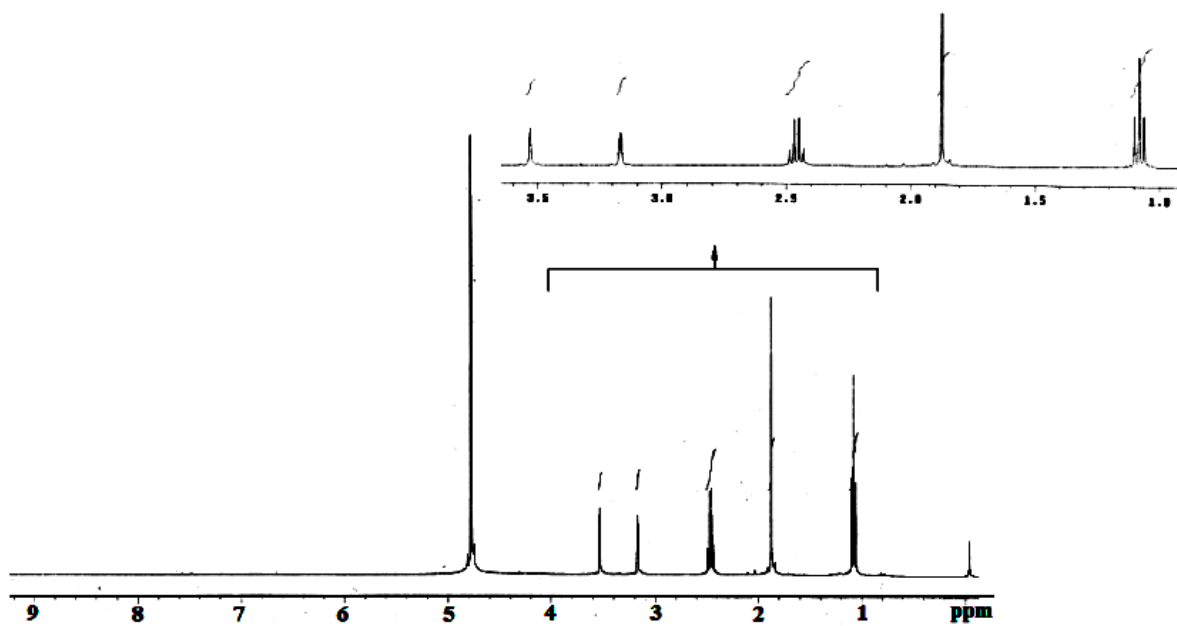


Figure S4: ^1H -NMR spectrum of **L** in methanol- d_4 .

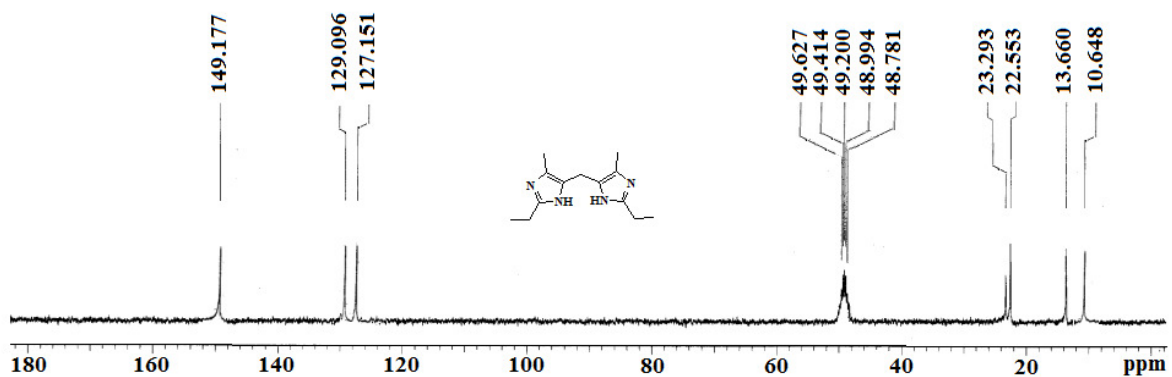


Figure S5: ^{13}C -NMR spectrum of **L** in methanol- d_4 .

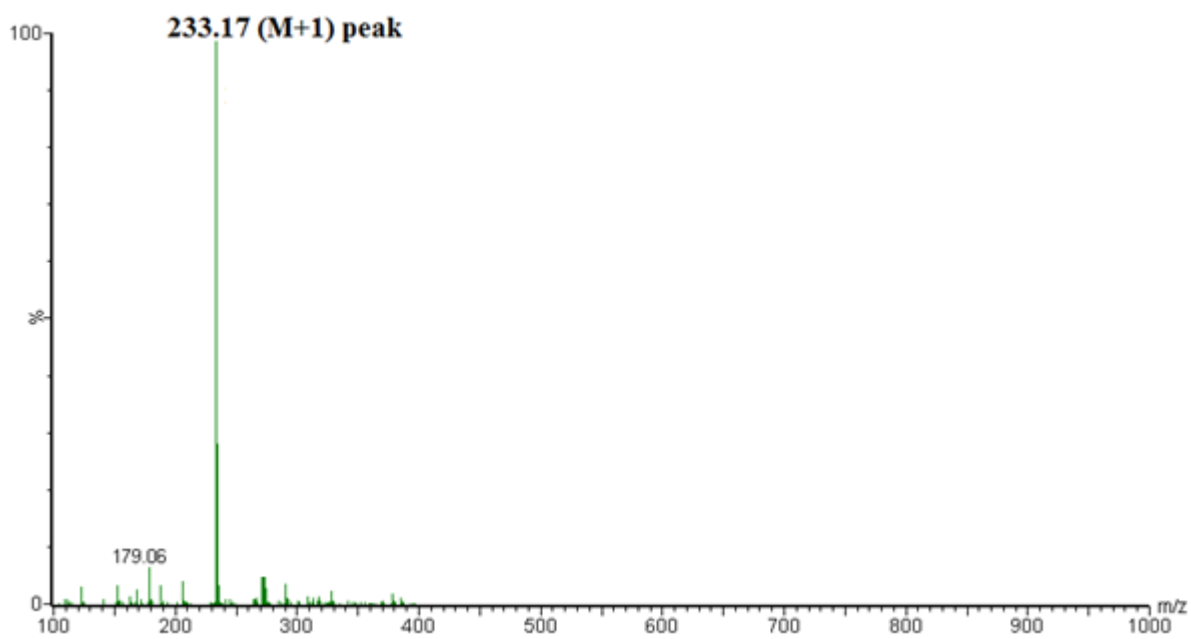


Figure S6: ESI-mass spectrum of **L** in methanol.

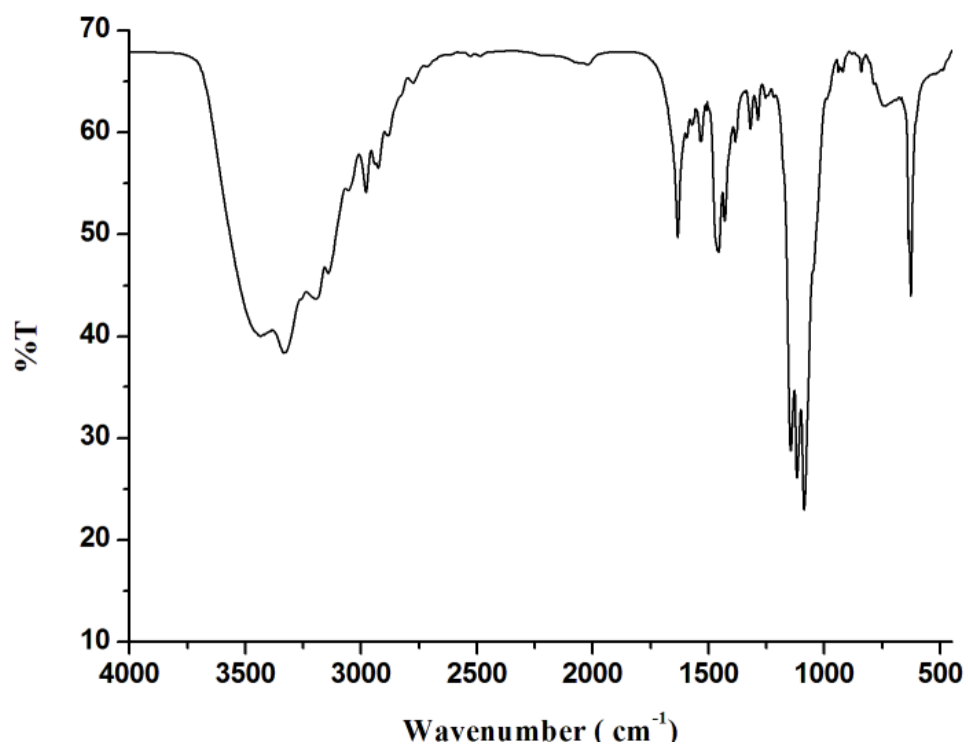


Figure S7: FT-IR spectrum of complex **1** in KBr.

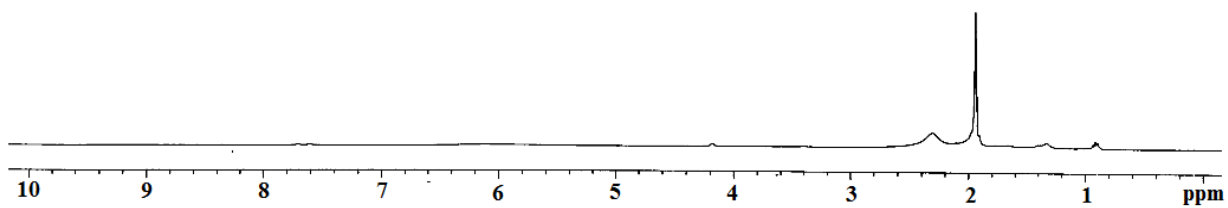


Figure S8: ¹H-NMR spectrum of complex **1** in CD₃CN.

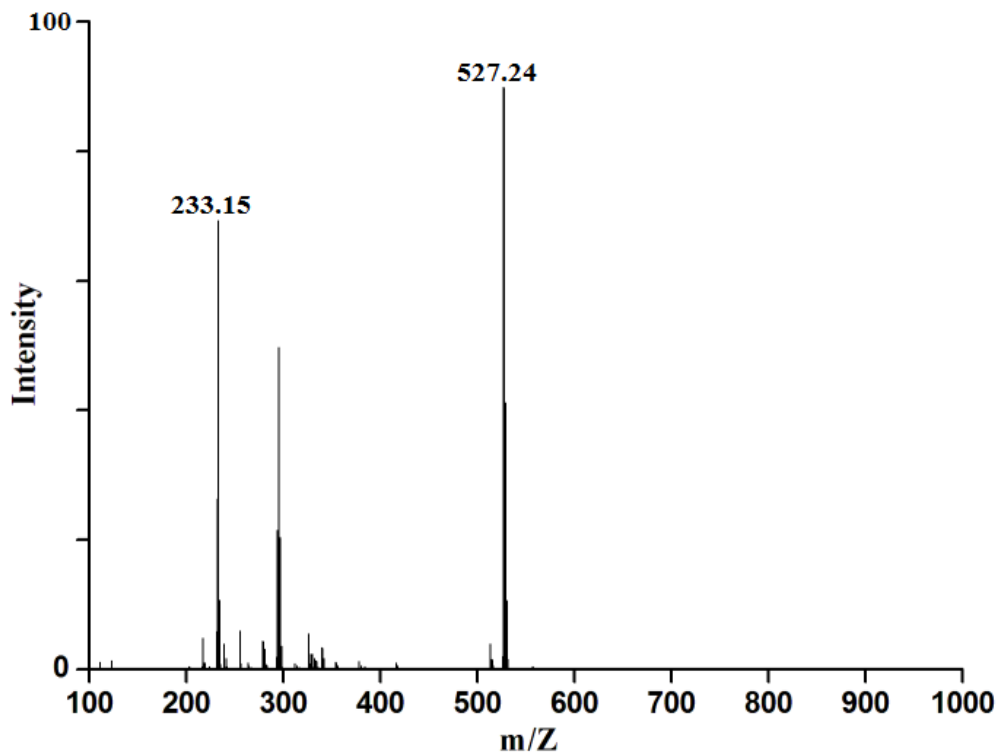


Figure S9: ESI-Mass spectrum of complex **1** in methanol.

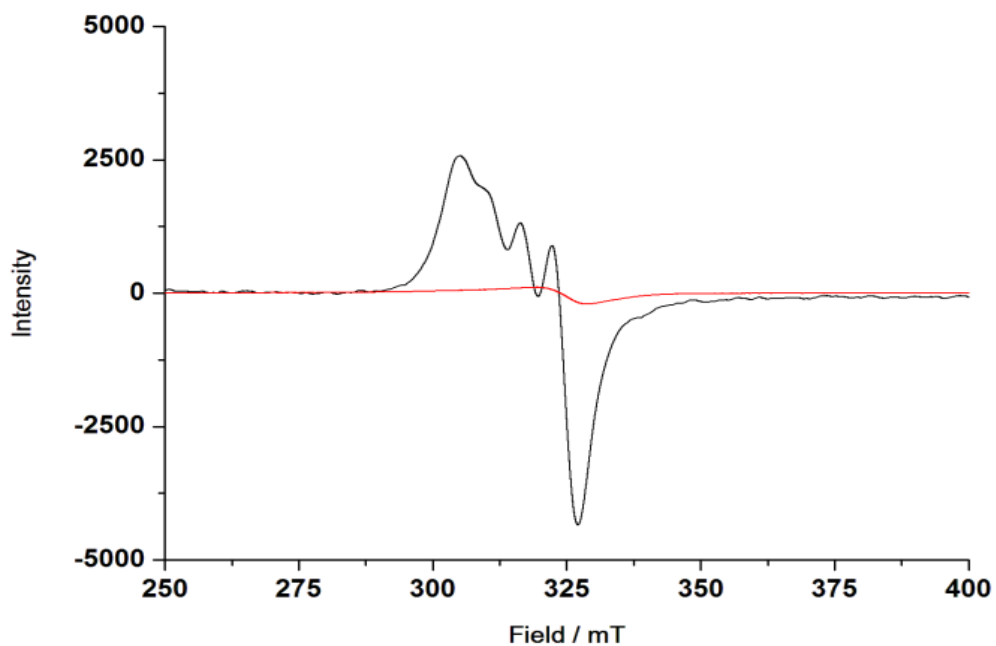


Figure S10: X-band EPR spectra of the complexes **1** (black) and **2** (red) in acetonitrile at 77 K.

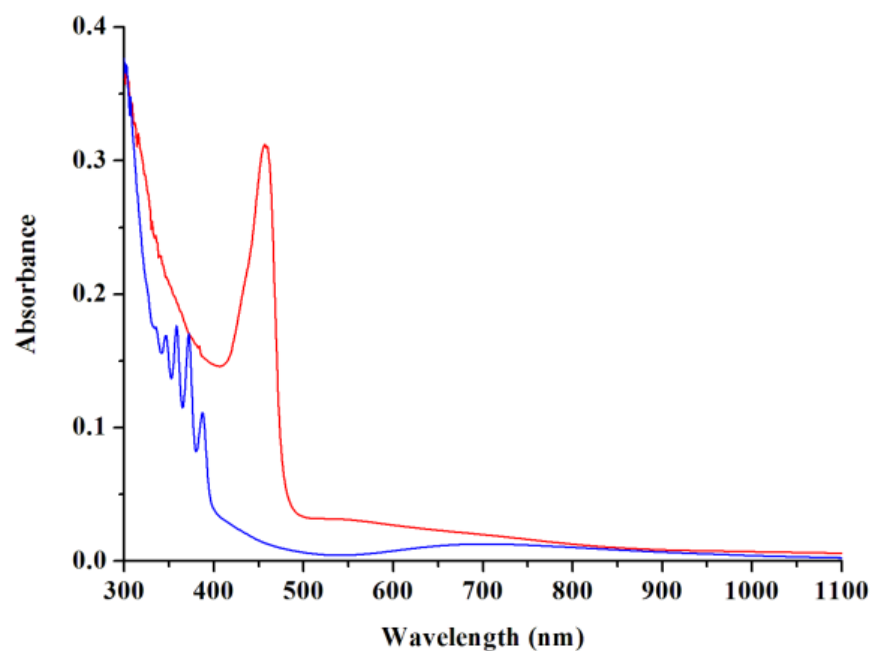


Figure S11: UV-visible spectra of complexes **1** (red) and **2** (blue) in acetonitrile solvent at room temperature.

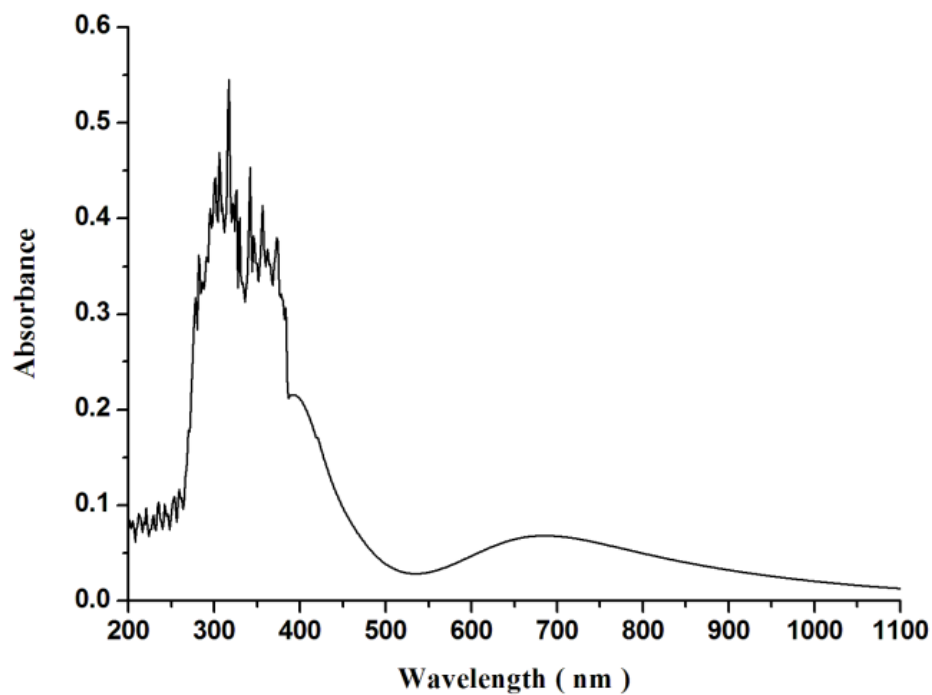


Figure S12: UV-visible spectrum of complex **2** in acetonitrile solvent at room temperature.

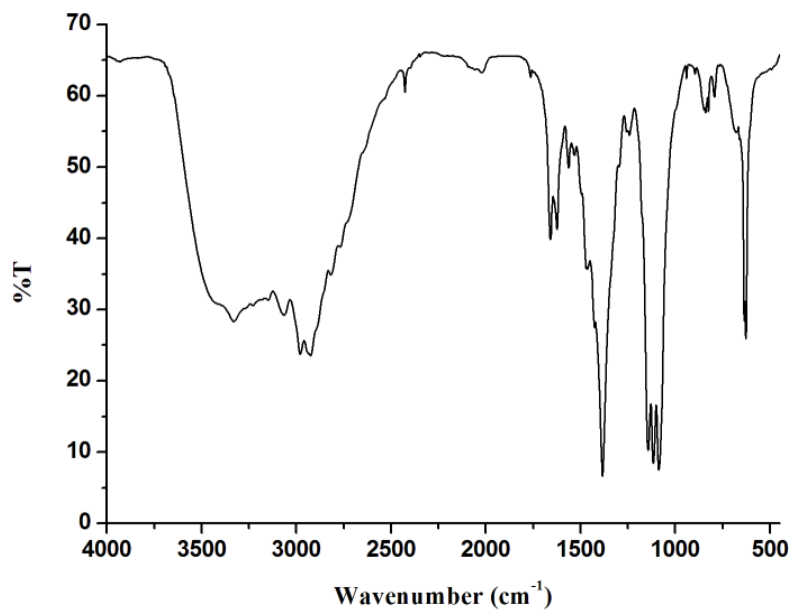


Figure S13: FT-IR spectrum of complex **2** in KBr.

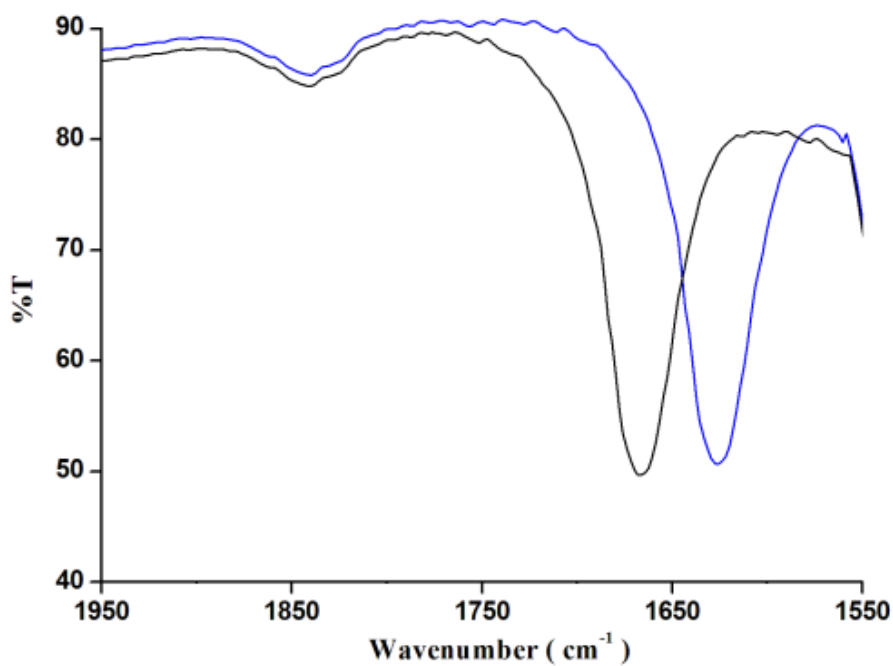


Figure S14: FT-IR spectra of complex **2** derived from nitric oxide (black) and ^{15}NO (blue) in acetonitrile solution. Only ν_{NO} frequency is shown for clarity.

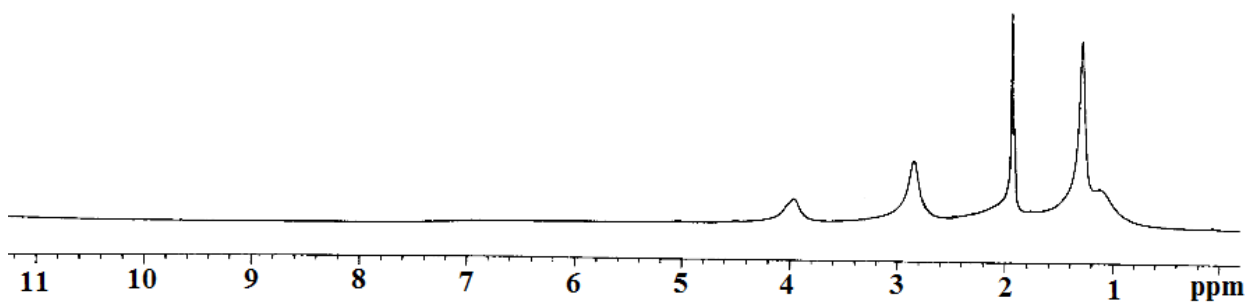


Figure S15: ¹H-NMR spectrum of complex **2** in CD₃CN.

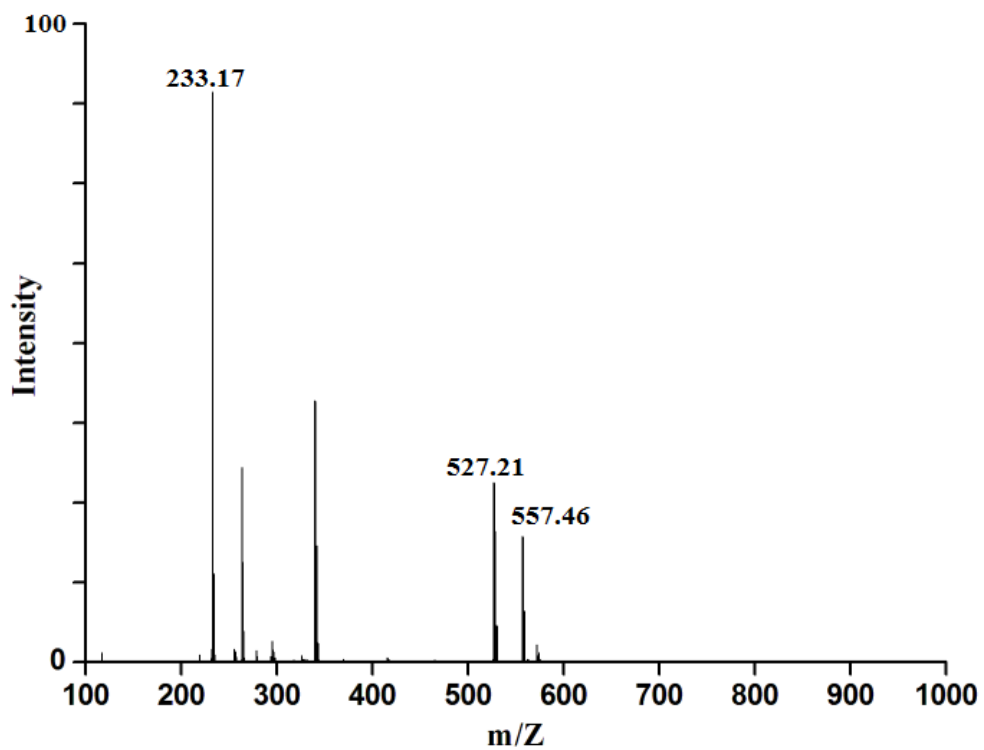


Figure S16: ESI-Mass spectrum of complex **2** in acetonitrile.

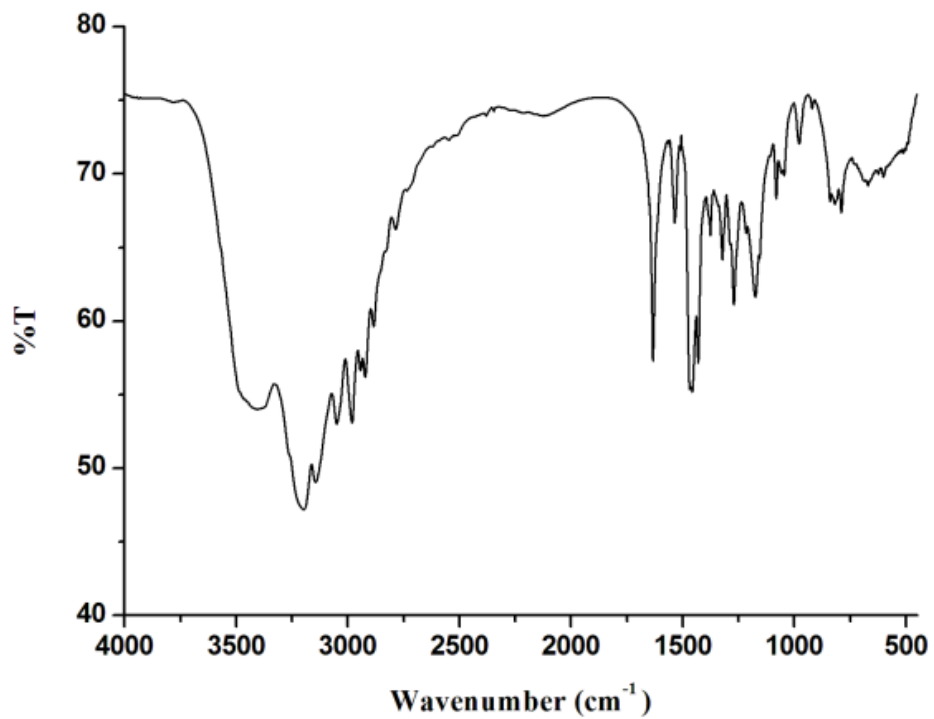


Figure S17: FT-IR spectrum of complex **3** in KBr.

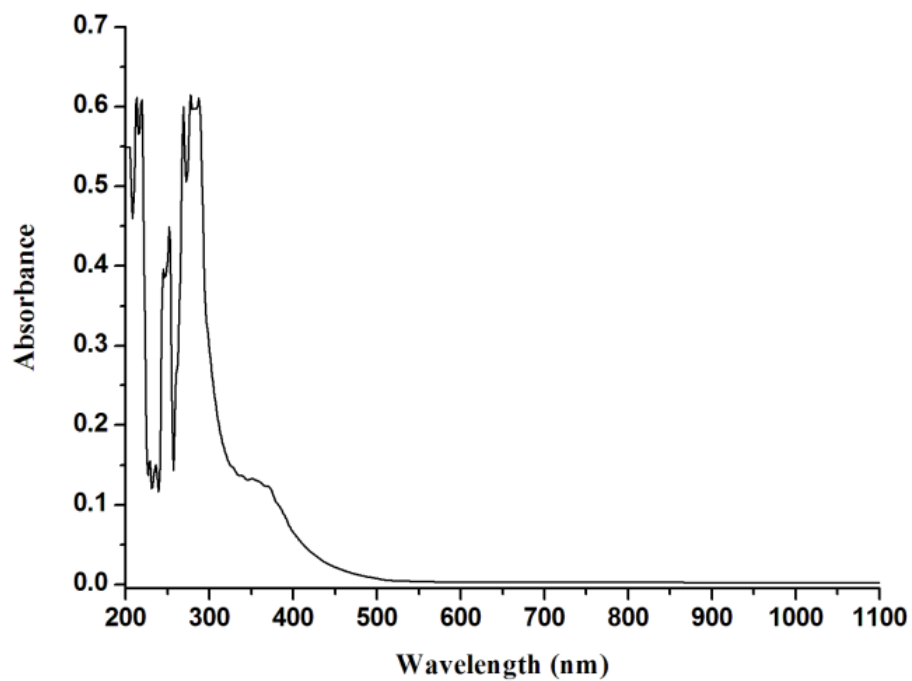


Figure S18: UV-visible spectrum of complex **3** in acetonitrile solvent at room temperature.

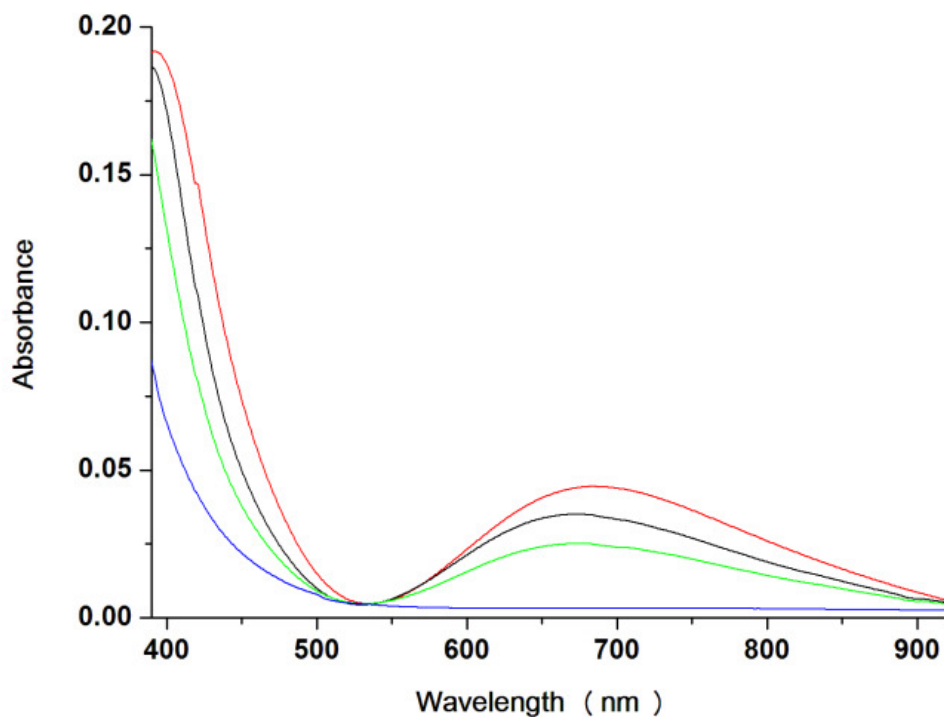


Figure S19: (a) UV-visible spectroscopic monitoring of the reaction of complex **2** with water in acetonitrile. Red and blue traces represent complexes **2** and **3**, respectively; whereas, black and green ones represent the intermediate steps for the gradual decomposition of complex **2** to **3**.

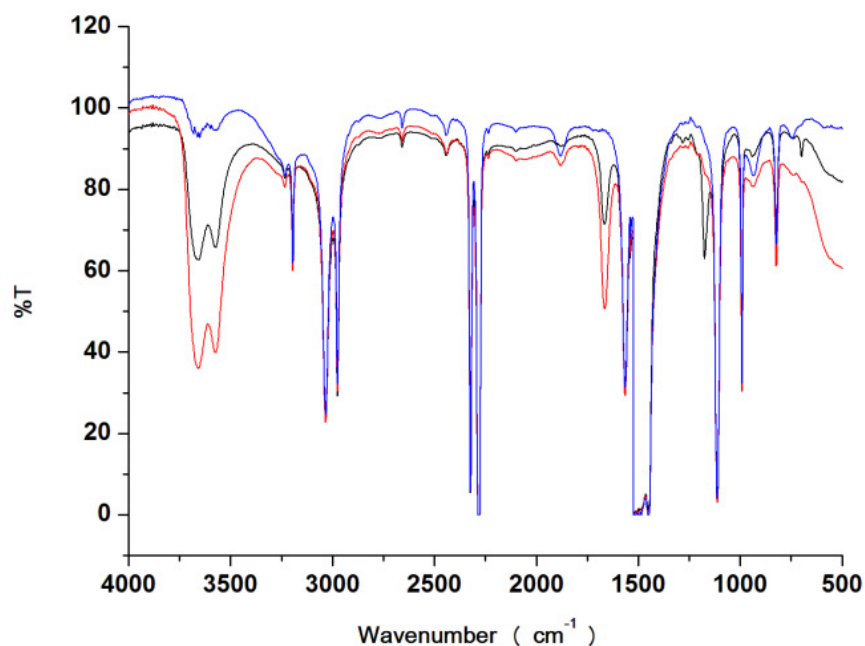


Figure S20: Solution FT-IR spectra of complex **2** (red line) and after reaction with water in acetonitrile solvent at room temperature.

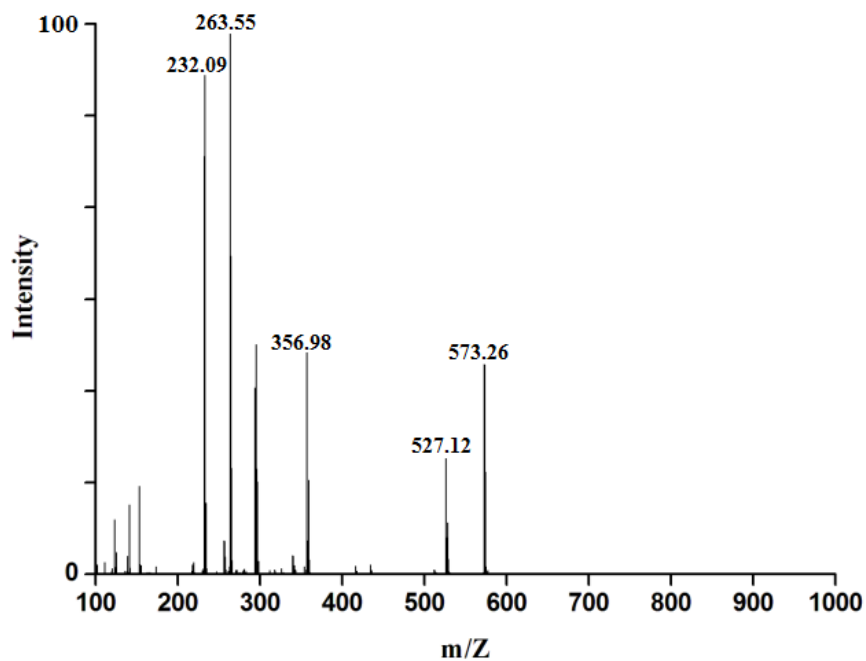


Figure S21: ESI-mass spectrum of complex **3** obtained from the reaction of complex **2** and water in acetonitrile.

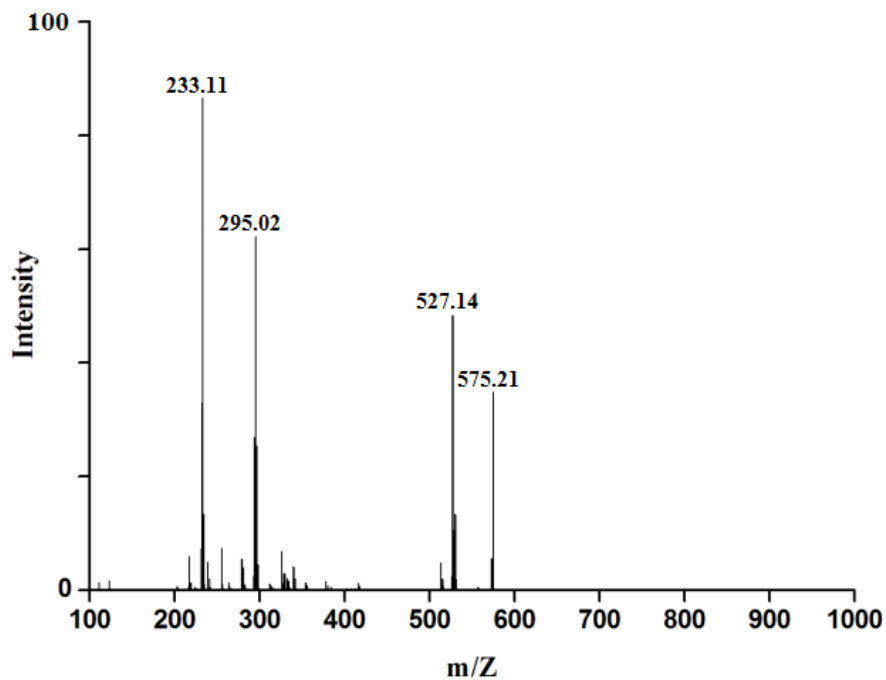


Figure S22: ESI-mass spectrum of complex **3** obtained from the reaction of complex **2** and water (^{18}O -labeled) in acetonitrile.

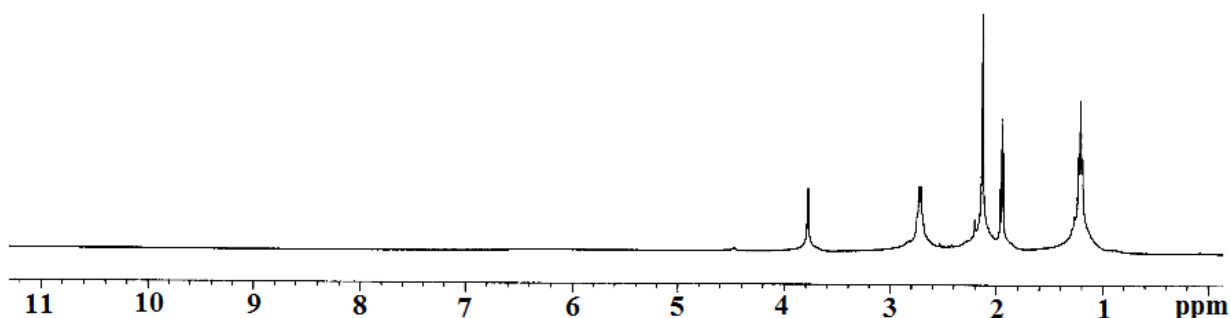


Figure S23: $^1\text{H-NMR}$ spectrum of complex **3** in CD_3CN .

Table S1. Crystallographic data for complexes **1** and **3**.

	Complex1	Complex 3
Formulae	$\text{C}_{30} \text{H}_{42} \text{Cl}_2 \text{Cu N}_{10} \text{O}_8$	$\text{C}_{26} \text{H}_{36} \text{Cu N}_9 \text{O}_6$
Mol. wt.	805.19	634.19
Crystal system	Triclinic	Monoclinic
Space group	P -1	P 2/c
Temperature /K	296(2)	296(2)
Wavelength /Å	0.71073	0.71073
$a / \text{Å}$	9.3488(6)	9.4710(2)
$b / \text{Å}$	11.1223(7)	9.4545(2)
$c / \text{Å}$	18.8929(11)	18.3295(5)
$\alpha / ^\circ$	77.839(3)	90.00
$\beta / ^\circ$	86.532(3)	90.0540(10)
$\gamma / ^\circ$	82.881(3)	90.00
$V / \text{Å}^3$	1904.4(2)	1641.29(7)
Z	2	2
$D_{\text{calc}} / \text{Mgm}^{-3}$	1.404	1.283
μ / mm^{-1}	0.773	0.716
Abs. correction	None	None
F(000)	838	664.0
Total no. of reflections	9262	4113
Reflections, $I > 2\sigma(I)$	6429	3330
Max. $2\theta / ^\circ$	28.32	28.38
Ranges (h, k, l)	-12 ≤ h ≤ 12 -14 ≤ k ≤ 14 -24 ≤ l ≤ 24	-12 ≤ h ≤ 12 -12 ≤ k ≤ 12 -24 ≤ l ≤ 24
Complete to 2θ (%)	97.5	99.8
Refinement method	Full-matrix least-squares on F^2	Full-matrix least-squares on F^2

Goof (F^2)	1.039	1.100
R indices [$I > 2\sigma(I)$]	0.0576	0.0582
R indices (all data)	0.0847	0.0674

Table S2. Selected bond length (Å) for complexes **1** and **3**.

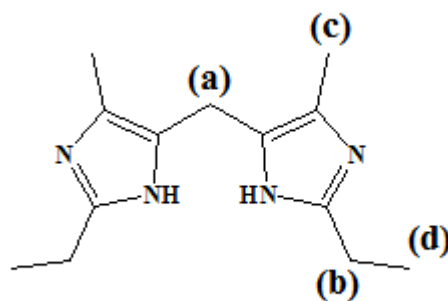
	Complex 1	Complex 3
Cu(1)-N(1)	2.035(2)	1.984(2)
Cu(1)-N(3)	1.995(3)	2.148(2)
Cu(1)-O(1)	-	2.353(3)
C(2)-C(1)	1.484(7)	1.530(5)
C(2)-C(3)	1.495(5)	1.488(4)
C(3)-N(1)	1.328(4)	1.329(3)
C(3)-N(2)	1.351(4)	1.353(4)
C(4)-N(2)	1.379(4)	1.380(4)
C(6)-N(1)	1.397(4)	1.401(3)
C(4)-C(5)	1.490(4)	1.507(5)
C(4)-C(6)	1.358(4)	1.340(4)
C(7)-C(6)	1.489(5)	1.486(4)
C(7)-C(8)	1.490(5)	1.501(4)
N(9)-O(1)	-	1.263(4)
C(9)-C(10)	1.493(5)	1.482(5)
C(11)-C(12)	1.489(5)	1.500(4)
C(12)-C(13)	1.49(1)	1.514(6)

Table S3. Selected bond angles (°) for complexes **1** and **3**.

	Complex 1	Complex 3
N(1)-Cu(1)-N(3)	86.7(1)	89.15(9)
Cu(1)-N(1)-C(3)	133.4(2)	129.4(2)
Cu(1)-N(1)-C(6)	119.7(2)	124.5(2)
Cu(1)-N(3)-C(8)	121.0(2)	120.0(2)
Cu(1)-N(3)-C(11)	131.5(2)	132.0(2)
N(1)-Cu(1)-O(1)	-	86.30(9)
N(3)-Cu(1)-O(1)	-	158.59(9)
C(1)-C(2)-C(3)	114.1(4)	113.5(3)
N(2)-C(3)-N(1)	109.2(3)	110.1(2)
C(3)-N(2)-C(4)	109.3(3)	107.9(3)
C(3)-N(1)-C(6)	106.9(3)	106.0(2)
C(5)-C(4)-C(6)	132.4(3)	132.3(3)

C(4)-C(6)-C(7)	130.8(3)	130.8(2)
C(6)-C(7)-C(8)	109.3(3)	111.9(2)
C(8)-C(9)-C(10)	132.0(3)	132.2(3)
C(8)-N(3)-C(11)	107.0(3)	106.0(2)
C(12)-C(11)-N(3)	128.3(3)	127.4(3)
C(11)-C(12)-C(13)	113.8(4)	114.6(3)

Table S4: NMR data



Chemical Shift (δ_{ppm})	Ligand (L)	Complex 2	Complex 3
(a)	3.53	3.96	3.77
(b)	2.59	2.84	2.71
(c)	1.87	1.91	1.92
(d)	1.08	1.28	1.21

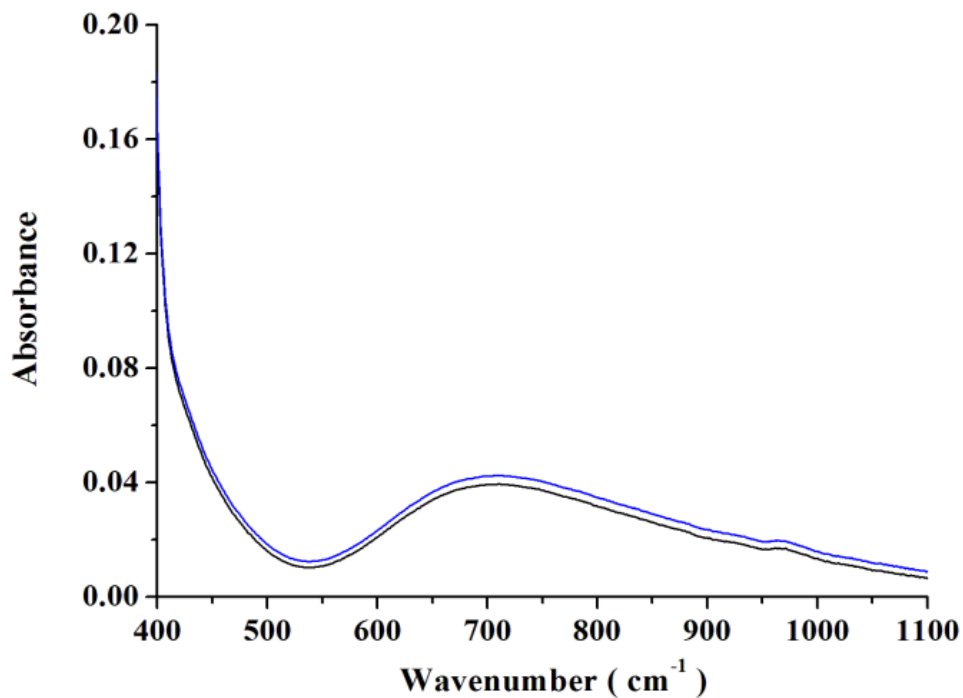


Figure S24: UV-visible spectra of complex **2** in degassed acetonitrile solution before (black trace) and after (blue trace) purging O₂ gas.

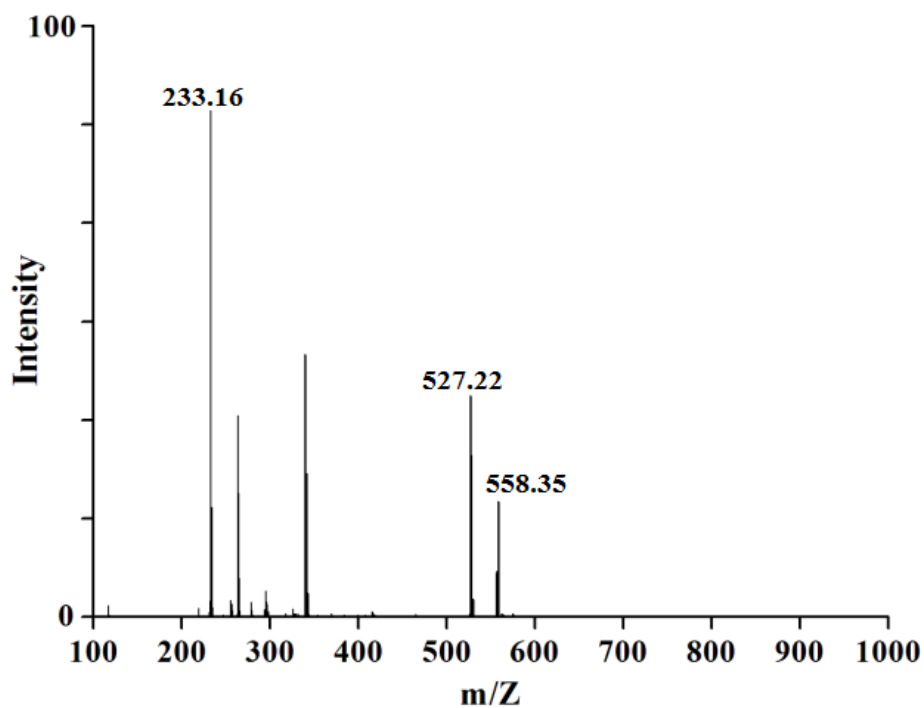


Figure S25: ESI-Mass spectrum of ¹⁵NO labeled complex **2** in methanol.

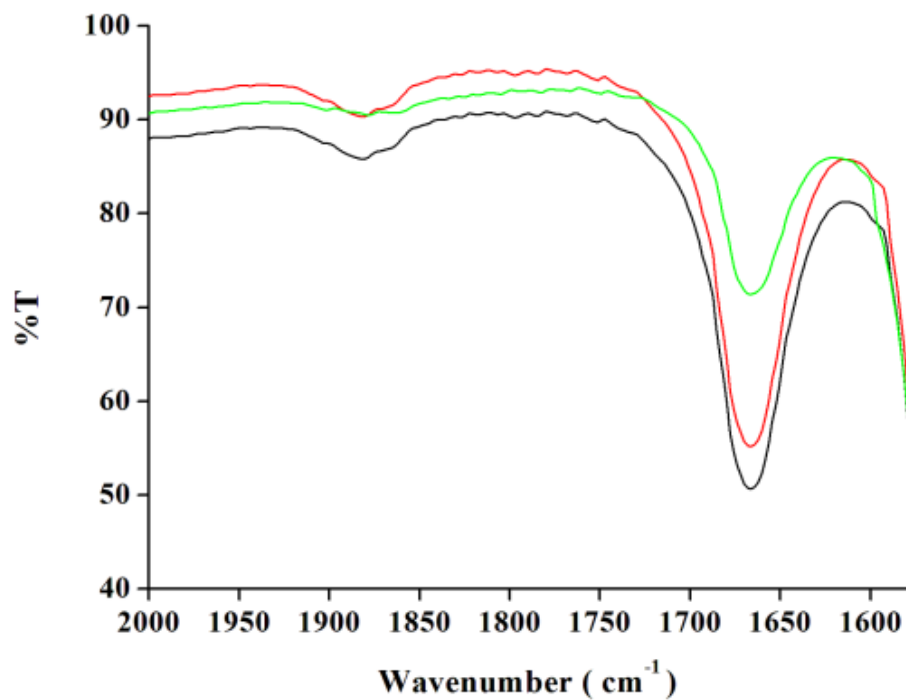


Figure S26: FT-IR spectra of complex **2** in acetonitrile solution before (black) and after applying vacuum [at 5 minutes (red) and 15 minutes (green)].

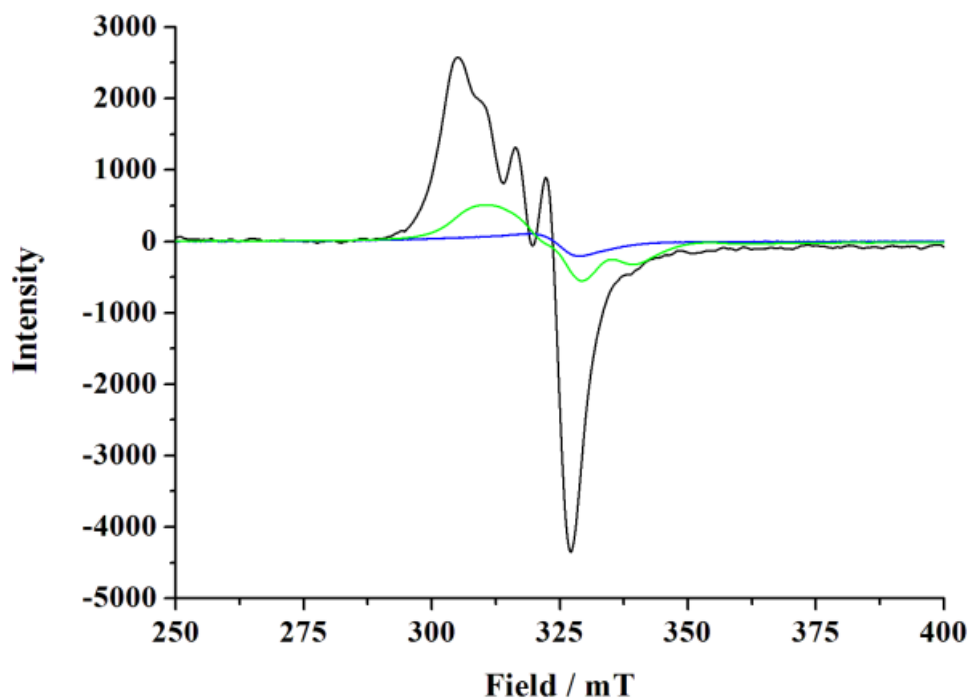


Figure S27: X-band EPR spectra of the complex **1** (black trace), complex **2** (blue trace) and after applying vacuum (green trace) upon the solution of complex **2** for 15 minutes in acetonitrile at room temperature.

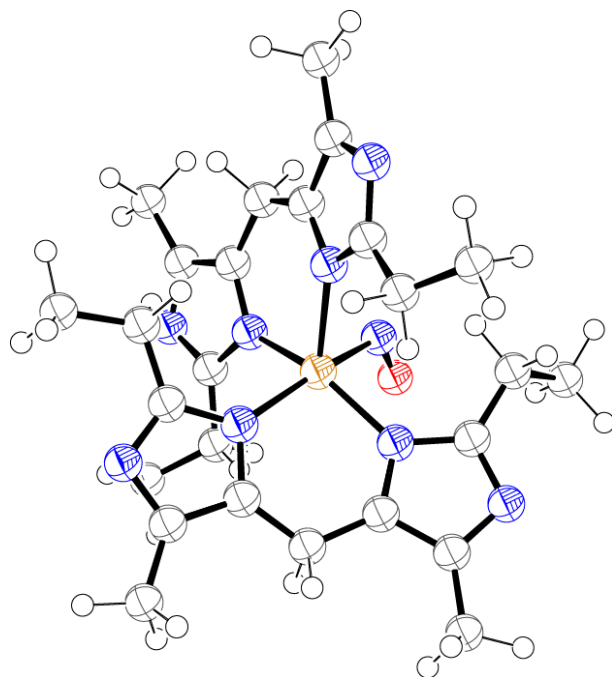


Figure S28: DFT optimized structure of complex **2** [Atom scheme: Blue, nitrogen; red, Oxygen; gray, Carbon; yellow, Copper].

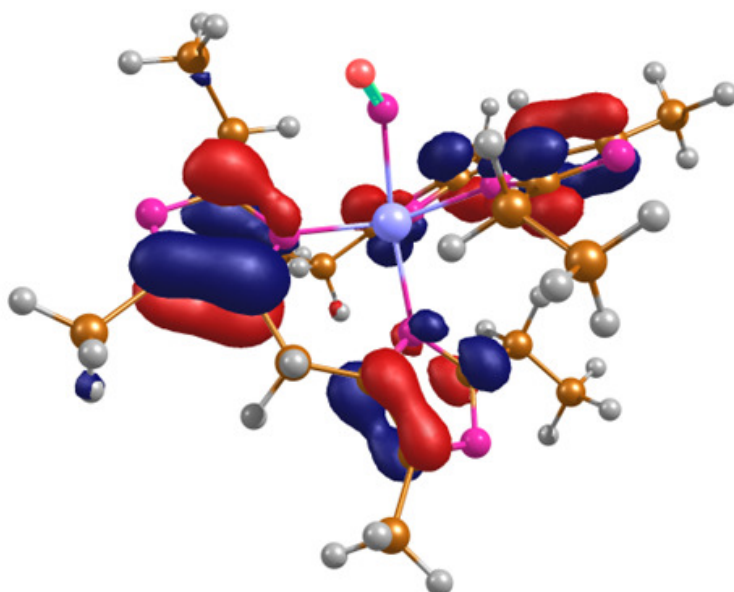


Figure S29: HOMO of complex **2**.

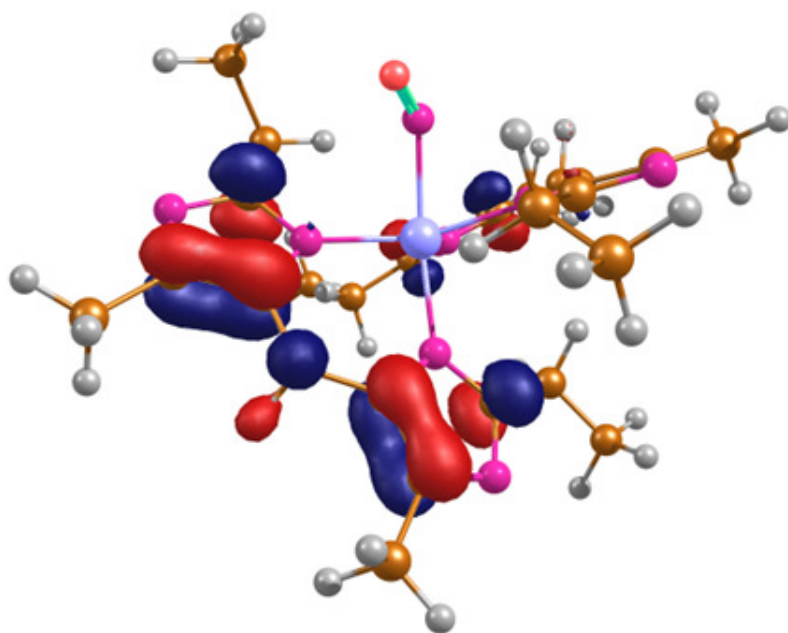


Figure S30: LUMO of complex **2**.

Table S5. Cartesian coordinates for complex **2**.

Cu1	2.716603511	2.876433295	4.604014134
N1	3.183577821	1.323807725	3.339529353
N2	3.993739068	-0.676064024	2.551807049
N3	1.383313896	3.606148654	3.337232189
N4	-0.154415958	4.927548724	2.278593267
N5	3.147758964	1.902519541	6.318285709
N6	3.108649884	0.362126237	7.993790082
N7	4.551544026	3.999869432	4.704374858
N8	6.205601167	5.568070712	4.347110036
C1	4.230125943	0.399050374	3.343703523
C2	2.785949867	-0.468740984	2.010410573
C3	2.136049059	-1.377297459	1.051627029
H1	1.116077603	-1.633161993	1.374207924
H2	2.723272122	-2.291916288	0.929472411
H3	2.031470402	-0.889113304	0.069360238
C4	2.275804526	0.812350432	2.501320093
C5	5.479739375	0.610081768	4.098347994
H4	5.900186302	1.577668346	3.772113684

H5	5.214691403	0.782369081	5.156059667
C6	6.515523334	-0.501851553	3.977186006
H6	6.114516519	-1.456177697	4.338795842
H7	7.397350959	-0.245895916	4.575699506
H8	6.830064770	-0.636778555	2.935693435
C7	1.013041370	1.442283655	2.093019087
H9	0.904386722	1.319076917	1.000793892
H10	0.172799423	0.819674479	2.471087710
C8	0.737313273	2.845597617	2.426838614
C9	-0.248717680	3.688750037	1.774650896
C10	0.828797386	4.874624324	3.208251157
C11	1.282191402	6.068945214	3.953203852
H11	1.715063063	6.766170419	3.215147807
H12	2.100647630	5.812138071	4.638744103
C12	0.147691160	6.804017908	4.688237551
H13	-0.313620060	6.166464005	5.452599326
H14	-0.633216480	7.109436023	3.982763540
H15	0.553948944	7.698485195	5.173277603
C13	-1.188262268	3.298202715	0.705619576
H16	-1.907579834	4.101367640	0.521439766
H17	-0.643669174	3.095150047	-0.230588445
H18	-1.723258972	2.373374680	0.962808270
C14	5.131734821	4.904671590	3.826383050
C15	6.347970139	5.088945787	5.581945607
C16	7.403889958	5.499006022	6.522439441
H19	8.058461616	4.646449202	6.763205308
H20	6.970608528	5.831642535	7.477184220
H21	8.009056378	6.302703145	6.094285954
C17	5.299774414	4.073375913	5.807746664
C18	5.170252737	3.261807241	7.022824075
H22	6.170497181	2.856704848	7.267627722
H23	5.012304189	3.960607119	7.873008540
C19	4.188149919	2.172890027	7.145420541
C20	4.152581373	1.188163115	8.203489809
C21	2.503740254	0.805661581	6.871150249
C22	1.271537335	0.226099744	6.296340555
H24	0.415122794	0.684474648	6.826959511
H25	1.173255498	0.553312647	5.252681837
C23	1.173380796	-1.298372946	6.414636324
H26	1.208644817	-1.613939852	7.463154861
H27	1.997979627	-1.785989286	5.879284925
H28	0.226074354	-1.636807463	5.980311550
C24	5.091168383	1.055294816	9.335452737
H29	6.072934872	0.701079662	8.981808571
H30	4.707315544	0.336230142	10.065613469
H31	5.264562073	2.022165807	9.827350383

C25	4.669164108	5.063822050	2.438409635
H32	5.248690216	4.330022842	1.841533996
H33	3.630330224	4.717650144	2.361223057
C26	4.867133335	6.455492806	1.832574847
H34	5.920359544	6.755273776	1.862469440
H35	4.279981381	7.205818475	2.376506662
H36	4.537173084	6.446535234	0.787585659
N9	1.907596660	4.000049785	6.122397871
O1	0.801298487	3.877335116	6.389540201

Table S6: Charge partitioning by Hirshfeld method for complex **2**

Cu	1 charge	0.3694
N	2 charge	-0.1305
N	3 charge	-0.1782
N	4 charge	-0.1281
N	5 charge	-0.1854
N	6 charge	-0.1242
N	7 charge	-0.1815
N	8 charge	-0.1406
N	9 charge	-0.1810
C	10 charge	0.1435
C	11 charge	0.1024
C	12 charge	-0.0822
H	13 charge	0.0769
H	14 charge	0.0673
H	15 charge	0.0799
C	16 charge	0.0851
C	17 charge	-0.0461
H	18 charge	0.0640
H	19 charge	0.0454
C	20 charge	-0.0983
H	21 charge	0.0429
H	22 charge	0.0528
H	23 charge	0.0435
C	24 charge	-0.0287
H	25 charge	0.1002
H	26 charge	0.1120
C	27 charge	0.0840
C	28 charge	0.0938
C	29 charge	0.1285
C	30 charge	-0.0511
H	31 charge	0.0754
H	32 charge	0.0357
C	33 charge	-0.0915

H	34 charge	0.0383
H	35 charge	0.0461
H	36 charge	0.0583
C	37 charge	-0.0846
H	38 charge	0.0657
H	39 charge	0.0768
H	40 charge	0.0735
C	41 charge	0.1511
C	42 charge	0.1080
C	43 charge	-0.0818
H	44 charge	0.0800
H	45 charge	0.0782
H	46 charge	0.0676
C	47 charge	0.0931
C	48 charge	-0.0304
H	49 charge	0.1030
H	50 charge	0.1110
C	51 charge	0.0712
C	52 charge	0.0898
C	53 charge	0.1266
C	54 charge	-0.0493
H	55 charge	0.0734
H	56 charge	0.0367
C	57 charge	-0.0949
H	58 charge	0.0426
H	59 charge	0.0422
H	60 charge	0.0549
C	61 charge	-0.0856
H	62 charge	0.0762
H	63 charge	0.0652
H	64 charge	0.0724
C	65 charge	-0.0434
H	66 charge	0.0831
H	67 charge	0.0424
C	68 charge	-0.0939
H	69 charge	0.0428
H	70 charge	0.0453
H	71 charge	0.0553
N	72 charge	0.1354
O	73 charge	0.1036

Table S7: Mulliken atomic charges

	charge
Cu(1)	0.427
N (2)	-0.402
N (3)	-0.327
N (4)	-0.440
N (5)	-0.327
N (6)	-0.439
N (7)	-0.327
N (8)	-0.422
N (9)	-0.326
C (10)	0.344
C (11)	0.164
C (12)	-0.340
H (13)	0.158
H (14)	0.154
H (15)	0.163
C (16)	0.223
C (17)	-0.279
H (18)	0.179
H (19)	0.171
C (20)	-0.283
H (21)	0.121
H (22)	0.125
H (23)	0.123
C (24)	-0.320
H (25)	0.223
H (26)	0.236
C (27)	0.248
C (28)	0.156
C (29)	0.342
C (30)	-0.323
H (31)	0.194
H (32)	0.160
C (33)	-0.268
H (34)	0.119
H (35)	0.133
H (36)	0.131
C (37)	-0.342
H (38)	0.152
H (39)	0.161
H (40)	0.153
C (41)	0.346

C (42) 0.171
C (43) -0.338
H (44) 0.162
H (45) 0.159
H (46) 0.154
C (47) 0.225
C (48) -0.319
H (49) 0.226
H (50) 0.241
C (51) 0.206
C (52) 0.158
C (53) 0.354
C (54) -0.287
H (55) 0.182
H (56) 0.147
C (57) -0.280
H (58) 0.128
H (59) 0.115
H (60) 0.127
C (61) -0.340
H (62) 0.160
H (63) 0.151
H (64) 0.151
C (65) -0.286
H (66) 0.190
H (67) 0.165
C (68) -0.284
H (69) 0.130
H (70) 0.119
H (71) 0.127
N (72) 0.171
O (73) 0.076

Results from NBO Analysis:

The NBO analysis⁴ which is given below show that the Cu atom in the complex has the following electronic configuration:

Cu 1 [core]4S(0.31)3d(9.37)5S(0.01)

Although the occupancies of the atomic orbitals are non-integer in the complex, the effective atomic configurations can be related to idealized atomic states. The Cu atom has an electronic configuration, [core] (4s)^{0.31}(3d)^{9.37}(5s)^{0.01} in the complex which is ideally a (3d)⁹ configuration representing copper to be at Cu (II) state. The NBO analysis is carried out with the GAUSSIAN 03 program¹ using B3LYP functional and 6-311G(d,p) basis set. The excess electrons shown in the configuration are due to the use of polarized basis set. The results of NBO analysis are given below:

Atom	No	Natural Electron Configuration
Cu	1	[core]4S(0.31)3d(9.37)5S(0.01)
N	2	[core]2S(1.39)2p(4.28)3p(0.02)
N	3	[core]2S(1.41)2p(4.08)3p(0.01)3d(0.01)
N	4	[core]2S(1.37)2p(4.33)3p(0.02)
N	5	[core]2S(1.41)2p(4.08)3p(0.01)3d(0.01)
N	6	[core]2S(1.38)2p(4.30)3p(0.02)
N	7	[core]2S(1.41)2p(4.07)3p(0.01)3d(0.01)
N	8	[core]2S(1.40)2p(4.29)3p(0.02)3d(0.01)
N	9	[core]2S(1.41)2p(4.08)3p(0.01)3d(0.01)
C	10	[core]2S(0.83)2p(2.57)3p(0.02)3d(0.01)
C	11	[core]2S(0.87)2p(2.79)3p(0.01)3d(0.01)
C	12	[core]2S(1.09)2p(3.54)3p(0.01)
H	13	1S(0.76)
H	14	1S(0.74)
H	15	1S(0.75)
C	16	[core]2S(0.85)2p(2.87)3p(0.02)3d(0.01)
C	17	[core]2S(1.02)2p(3.42)3p(0.01)
H	18	1S(0.76)
H	19	1S(0.76)
C	20	[core]2S(1.09)2p(3.47)3p(0.01)
H	21	1S(0.78)
H	22	1S(0.79)
H	23	1S(0.78)
C	24	[core]2S(1.00)2p(3.50)3p(0.01)
H	25	1S(0.70)
H	26	1S(0.68)
C	27	[core]2S(0.84)2p(2.89)3p(0.02)3d(0.01)
C	28	[core]2S(0.86)2p(2.83)3p(0.01)3d(0.01)
C	29	[core]2S(0.82)2p(2.62)3p(0.02)3d(0.01)
C	30	[core]2S(1.02)2p(3.42)3p(0.01)
H	31	1S(0.74)
H	32	1S(0.79)
C	33	[core]2S(1.09)2p(3.45)
H	34	1S(0.80)
H	35	1S(0.77)
H	36	1S(0.78)
C	37	[core]2S(1.09)2p(3.54)3p(0.01)
H	38	1S(0.74)
H	39	1S(0.76)
H	40	1S(0.77)
C	41	[core]2S(0.83)2p(2.55)3p(0.02)3d(0.01)
C	42	[core]2S(0.87)2p(2.79)3p(0.02)3d(0.01)

```
C 43      [core]2S( 1.09)2p( 3.54)3p( 0.01)
H 44          1S( 0.75)
H 45          1S( 0.76)
H 46          1S( 0.74)
C 47      [core]2S( 0.85)2p( 2.85)3p( 0.02)3d( 0.01)
C 48      [core]2S( 1.00)2p( 3.51)3p( 0.01)
H 49          1S( 0.70)
H 50          1S( 0.68)
C 51      [core]2S( 0.84)2p( 2.93)3p( 0.02)3d( 0.01)
C 52      [core]2S( 0.86)2p( 2.83)3p( 0.01)3d( 0.01)
C 53      [core]2S( 0.81)2p( 2.62)3p( 0.02)3d( 0.01)
C 54      [core]2S( 1.02)2p( 3.41)3p( 0.01)
H 55          1S( 0.75)
H 56          1S( 0.80)
C 57      [core]2S( 1.09)2p( 3.46)3p( 0.01)
H 58          1S( 0.77)
H 59          1S( 0.80)
H 60          1S( 0.79)
C 61      [core]2S( 1.09)2p( 3.54)3p( 0.01)
H 62          1S( 0.76)
H 63          1S( 0.74)
H 64          1S( 0.77)
C 65      [core]2S( 1.02)2p( 3.42)3p( 0.01)
H 66          1S( 0.73)
H 67          1S( 0.78)
C 68      [core]2S( 1.09)2p( 3.46)3p( 0.01)
H 69          1S( 0.77)
H 70          1S( 0.80)
H 71          1S( 0.78)
N 72      [core]2S( 1.67)2p( 3.10)3S( 0.02)3p( 0.03)3d( 0.01)
O 73      [core]2S( 1.72)2p( 4.31)3S( 0.01)3p( 0.01)3d( 0.01)
```

Reference:

1. M. Shiri, M. A. Zolfigol, H. G. Kruger, Z. Tanbakouchian, *Chem. Rev.* 2010, **110**, 2250- 2293.
2. J. Andzelm, C. Koelmel, A. Klamt, *J. Chem Phys*, 1995, **103**, 9312–9320
3. B. Delly, *J. Chem. Phys.* 1990, **92**, 508-514.
4. M. J. Frisch, G. W. Trucks, H. B. Schlegel, G. E. Scuseria, M. A. Robb, J. R. Cheeseman, J. A. Montgomery Jr., T. Vreven, K. N. Kudin, J. C. Burant, J. M. Millam, S. S. Iyengar, J. Tomasi, V. Barone, B. Mennucci, M. Cossi, G. Scalmani, N. Rega, G. A. Petersson, H. Nakatsuji, M. Hada, M. Ehara, K. Toyota, R. Fukuda, J. Hasegawa, M. Ishida, T. Nakajima, Y. Honda, O. Kitao, H. Nakai, M. Klene, X. Li, J. E. Knox, H.P. Hratchian, J. B. Cross, V. Bakken, C. Adamo, J. Jaramillo, R. Gomperts, R. E. Stratmann, O. Yazyev, A. J. Austin, R. Cammi, C. Pomelli, J. W. Ochterski, P. Y. Ayala, K. Morokuma, G.A. Voth, P. Salvador, J. J. Dannenberg, V. G. Zakrzewski, S. Dapprich, A. D. Daniels, M. C. Strain, O. Farkas, D. K. Malick, A. D. Rabuck, K. Raghavachari, J. B. Foresman, J. V. Ortiz, Q. Cui, A. G. Baboul, S. Clifford, J. Cioslowski, B. B. Stefanov, G. Liu, A. Liashenko, P. Piskorz, I. Komaromi, R. L. Martin, D. J. Fox, T. Keith, M. A. Al-Laham, C. Y. Peng, A. Nanayakkara, M. Challacombe, P. M. W Gill, B. Johnson, W. Chen, M. W. Wong, C. Gonzalez, J. A. Pople, *Gaussian 03*, revision A.1; Gaussian, Inc.: Pittsburgh PA, 2003.